

1 Characterization of urban amine-containing particles in Southwestern China: seasonal
2 variation, source, and processing

3 Yang Chen^{1,2*}, Mi Tian¹, Rujin Huang², Guangming Shi⁴, Huanbo Wang¹, Chao Peng¹,
4 Junji Cao², Qiyuan Wang², Shumin Zhang³, Dongmei Guo³, Leiming Zhang⁵, and
5 Fumo Yang^{1,4,*}

6 ¹Research Center for Atmospheric Environment, Chongqing Institute of Green and
7 Intelligent Technology, Chinese Academy of Sciences, Chongqing 400714, China.

8 ²Key Lab of Aerosol Chemistry & Physics, State Key Laboratory of Loess and
9 Quaternary Geology, Institute of Earth Environment, Chinese Academy of Sciences,
10 Xi'an 710061, China.

11 ³School of Basic Medical Sciences, North Sichuan Medical College, Nanchong 637000,
12 Sichuan, China.

13 ⁴National Engineering Research Center for Flue Gas Desulfurization, Department of
14 Environmental Science and Engineering, Sichuan University, Chengdu 610065, China

15 ⁵Air Quality Research Division, Science and Technology Branch, Environment and
16 Climate Change Canada, Toronto M3H 5T4, Canada

17 Correspondence to: Yang Chen (chenyang@cigit.ac.cn); Fumo Yang
18 (fmyang@scu.edu.cn)

19 Keyword: single particle; amine; urban environment, processing

20

21

Abstract

22 Amine-containing particles were characterized in an urban area of Chongqing during
23 both summer and winter using a single particle aerosol mass spectrometer (SPAMS).
24 Among the collected particles, 12.7% were amine-containing in winter and 8.3% in
25 summer. Amines were internally mixed with elemental carbon (EC), organic carbon
26 (OC), sulfate, and nitrate. Diethylamine (DEA) was the most abundant among amine-
27 containing particles. Wintertime amine-containing particles were mainly from the
28 northwest direction where a forest park was located; in summer, they were from the
29 northwest and southwest (traffic hub) directions. These origins suggest that vegetation
30 and traffic were the primary sources of particulate amines. The average relative peak
31 area of DEA depended strongly on humidity, indicating that the enhancement of DEA
32 was possibly due to increasing aerosol water content and aerosol acidity. Using an
33 adaptive resonance theory neural network (ART-2a) algorithm, four major types of
34 amine-containing particles were clustered including amine-organic-carbon (A-OC), A-
35 OCEC, DEA-OC, and A-OCEC-aged. The identified particle types implied that amines
36 were **taken up** by particles produced from traffic and biomass burning. Knowledge
37 gained in this study is useful to understand the atmospheric processing, origin, and
38 sources of amine-containing particles in the urban area of Chongqing.

39

40 **1. Introduction**

41 Amines are ubiquitous in the atmosphere and have both natural (ocean, biomass burning,
42 and vegetation) and anthropogenic (animal husbandry, industry, combustion, and traffic)
43 emission sources (Ge et al., 2011a). Trimethylamine (TMA) is one of the most abundant
44 amines with an estimated global emission flux of 170Gg year⁻¹ (Ge et al., 2011a).
45 Gaseous amines compete with ammonia in acid-base reactions, participate in gas-
46 particle partitioning, and contribute to wet and dry deposition (Angelino et al., 2001;
47 Monks, 2005; Gómez Alvarez et al., 2007; De Haan et al., 2011; Huang et al., 2012;
48 You et al., 2014). Gaseous amines also play an essential role in new particle formation
49 via enhancing the ternary nucleation of H₂SO₄-H₂O clusters in remote areas (Bzdek et
50 al., 2012; Kirkby et al., 2011). In polluted areas, H₂SO₄-diethylamine (DMA)-water
51 clusters were important during the new particle formation events (Yao et al., 2018).
52 Amines are also essential in the growth of ambient particles. For example, particulate
53 aminium salts, which were produced via amine-acid neutralization, tended to prevent
54 the coagulation between pre-existing particles leading to increased particle number
55 concentrations (Wang et al., 2010; Smith et al., 2010). Moreover, the enrichment of
56 TMA had been observed in cloud and fog processing (Zhang et al., 2012; Rehbein et
57 al., 2011). Characterization of amine-containing particles is important to evaluate their
58 processing and impact.

59 Single particle mass spectrometers (SPMS), such as aerosol time-of-flight mass
60 spectrometer (ATOFMS) and Single Particle Aerosol Mass Spectrometer (SPAMS),
61 have been widely used in real-time measurements of amine-containing particles for
62 chemical composition and mixing state (Li et al., 2017). SPAMS is different from the
63 Aerodyne soot-particle aerosol mass spectrometer (SP-AMS), which is a type of

64 aerosol mass spectrometer (AMS) for detecting black carbon, sulfate, nitrate,
65 ammonium, chloride, and organics (Onasch et al., 2012; Wang et al., 2016). The
66 chemical composition and mixing state of TMA-containing particles have been
67 reported worldwide, such as in California, USA (Denkenberger et al., 2007; Qin et al.,
68 2012)); Ontario, Canada (Tan et al., 2002; Rehbein et al., 2011); Mexico City (Moffet
69 et al., 2008)); European cities (Barcelona, Cork, Zurich, Paris, Dunkirk and Corsica
70 (Healy et al., 2015; Dall'Osto et al., 2016)), and Chinese cities such as Guangzhou,
71 Shanghai and Xi'an (Zhang et al., 2012; Chen et al., 2016; Huang et al., 2012). In the
72 five European cities such as Cork, Paris, Dunkirk, Corsica, and Zurich, amines were
73 found internally mixed with sulfate and nitrate; but in Corsica, amines were internally
74 mixed with methanesulfonate (Healy et al., 2015). In Barcelona, five unique types of
75 amine-containing particles were observed, including *amine-POA58* (composed of
76 amines, sulfate, and nitrate), *amine-EST84*(environment tobacco smoke), *amine-*
77 *SOA59* (composed of TMA and organics), *amine-SOA114*, and organic nitrogen
78 amines (Dall'Osto et al., 2016; Dall'Osto et al., 2013). In a rural area site in the Pearl
79 River Delta (China), the marker ion, $(C_2H_5)_2NH_2^+$, was the most abundant (90% and
80 86% of amine-containing particles in summer and winter) (Cheng et al., 2018). In
81 Guangzhou, TMA-containing particles were important, taking up to 7% in number
82 fraction during clear days and 35% during fog events (Zhang et al., 2012). In previous
83 studies, reported high RH conditions and fog processing were favorable for the
84 enhancement of trimethylamine in the particle phase. Zhang et al. found that, during
85 fog events, the number fraction of TMA-containing particles took up to 35%; in the
86 size range of 0.5-2.0 μm , the fraction accounted up to 60% (Zhang et al., 2012). Thus
87 the location-specific studies in the varied environments are still necessary.

88 The knowledge of amine-containing particles is limited in southwestern China. In this
89 region, Chongqing is a megacity with a population of 8.23 million. The city is
90 subtropical, industrial, and polluted (Chen et al., 2017; Tao et al., 2017). Fog events
91 frequently occurred in this area, and hence, it is known as the “fog city” in China. The
92 effect of high relative humidity (RH) on the processing of amine-containing particles
93 needs investigation. This study aims to characterize the amine-containing particles,
94 including chemical composition, mixing state, atmospheric processing, and source in
95 Chongqing during winter and summer.

96 **2. Methods**

97 **2.1 Sampling site**

98 Ambient single particles were collected at an urban air quality supersite from
99 07/05/2016 to 08/14/2016 (referred to as a summer season) and from 01/21/2016 to
100 02/25/2016 (referred to as a winter season). The supersite has been described in our
101 previous studies (Chen et al., 2017). Briefly, the supersite is located on the rooftop of a
102 commercial office building (106.51°E, 29.62°N) at a height of 30 m above the ground
103 ([Figure S1](#)). The building is surrounded by business and residential communities and is
104 15 km from the city center. A 3 km² forest park is located northwest of the sampling
105 site and a traffic hub in the southwest.

106 **2.2 Instrumentation**

107 A SPAMS ([Hexin Inc. Guangzhou, China, model 0515](#)) was deployed for single
108 particle sampling, and the technical description of SPAMS is available in the literature
109 (Li et al., 2011; Chen et al., 2017). Briefly, after passing through a diffusive dryer,
110 particles in a size range of 0.1–2.0 μm are sampled via an aerodynamic lens and form

111 a particle beam. Particles in the beam come across two pre-positioned laser beams (Nd:
112 YAG, 532 nm) one-by-one, and the vacuum aerodynamic diameter (D_{va}) of each
113 particle is determined via its time-of-flight. Particles are ionized using an Nd: YAG
114 laser operating at a wavelength of 266 nm. The ions are analyzed using a bipolar time-
115 of-flight mass spectrometer. Due to the limitation of SPAMS, quantification of
116 particulate amines was not attempted.

117 **2.3 Data analysis**

118 The SPAMS data were imported into the YAADA toolkit (Software Toolkit to Analyze
119 Single-Particle Mass Spectral Data, v 2.11) to form a single particle dataset. The [query](#)
120 was conducted using the marker ions of amines.: m/z 59 $[(CH_3)_3N]^+$ (TMA), 74
121 $[(C_2H_5)_2NH_2]^+$ (diethylamine, DEA), 86 $[(C_2H_5)_2NCH_2]^+$ or $[C_3H_7NHC_2H_4]^+$ (DEA or
122 DPA), 101 $[(C_2H_5)_3N]^+$ (TEA), 102 $[(C_3H_7)_2NH_2]^+$ (DPA), 114 $[(C_3H_7)_2NCH_2]^+$ (DPA),
123 and 143 $[(C_3H_7)_3N]^+$ (TPA) (Healy et al., 2015). Firstly, m/z 59 was used for querying
124 the TMA-containing particles; m/z 74 for the DEA-containing particles and m/z 86 for
125 TEA-containing particles, and so on. [The query strategy resulted in duplicate particles](#)
126 [in the result when various amines co-existed in one single amine-containing particle.](#)
127 [After the duplicate particles were removed from the multiple query results described](#)
128 [above, all amine-containing particles were combined into an amine-containing particle](#)
129 [cluster.](#) Various amines could be both internally and externally mixed in these particle
130 clusters.

131 An adaptive resonance theory based neural network algorithm (ART-2a) was applied
132 to cluster the amine-containing particle types using a vigilance factor of 0.70, a learning
133 rate of 0.05, and 20 iterations (Song et al., 1999). This procedure produced 67 clusters
134 in summer and 75 clusters in winter; many of these clusters exhibited identical mass

135 spectra with slight differences in specific ion intensities. A well-established combining
136 strategy, on the basis of similar mass spectra, temporal trends, and size distribution, was
137 adopted to merge these particle clusters into the finalized particle types (Dallosto and
138 Harrison, 2006). In addition, the relative peak area (RPA) is defined as the peak area of
139 each m/z divided by the total dual-ion mass spectral peak areas of each particle (Healy
140 et al., 2013). To calculate the overall RPA of amines, the relative peak area of amines
141 in each particle were extracted and summed up.

142 **3. Results and discussion**

143 **3.1 Single particle chemical composition and seasonal variation**

144 The percentage of amine-containing particles was 12.7% in the winter SPAMS dataset
145 and 8.3% in the summer dataset. The DEA-containing particles were dominant,
146 accounting for 70% and 78% of all amine-containing particles in winter and summer,
147 respectively; while TMA-containing particles were minor, accounting for up to 7% in
148 winter and 3% in summer among all the amine-containing particles. The average mass
149 spectra of DEA-, DPA, and TMA-containing particles are provided in Figure S2, and
150 these spectra showed strong homogeneity. The determination coefficient (R^2) between
151 DEA- and DPA- containing particles was 0.98, and R^2 between DEA- and TMA-
152 containing particles was 0.83.

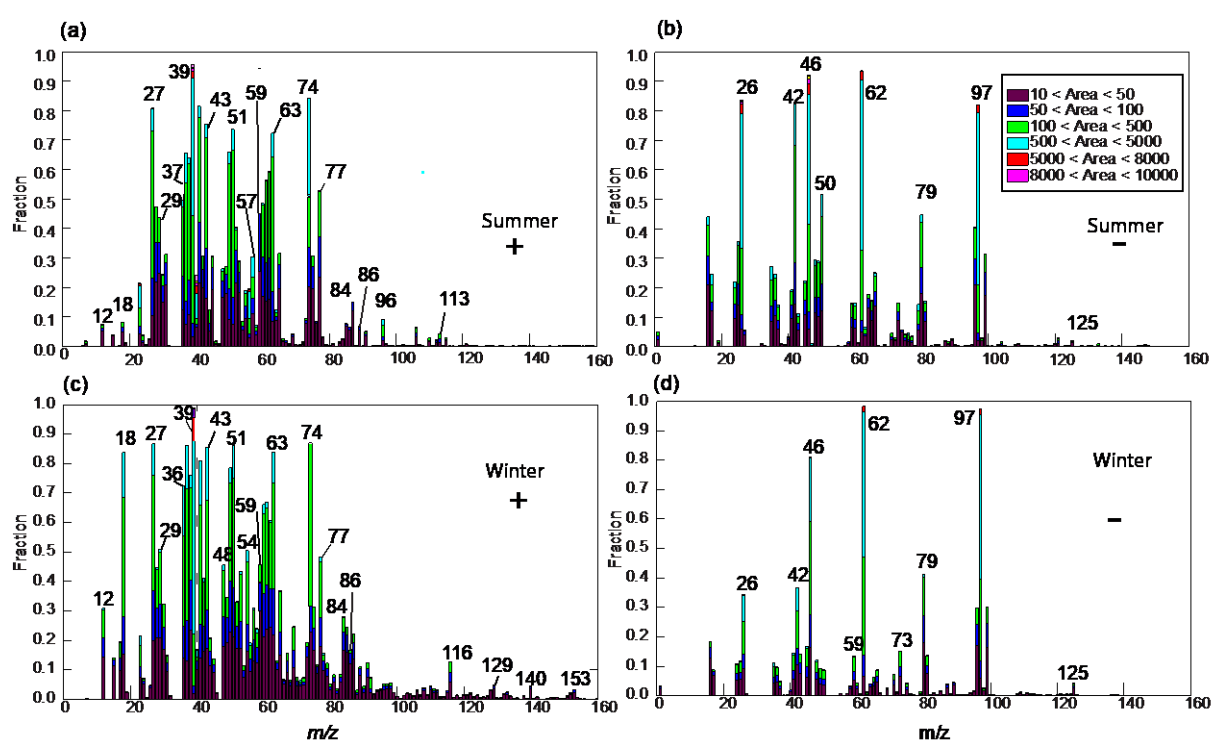
153 Figure 1 shows the digital mass spectra of amine-containing particles in two seasons.
154 In each spectrum, the ion height indicates its fraction in the amine-containing particle
155 dataset, and the stacked color map shows the corresponding ion intensity ranges. The
156 assignment of ions is shown in Table S1. In both seasons, the dominant ions were K^+
157 (m/z 39 and 41), amines (m/z 59, 74, and 86), and organics (m/z 43, 51, 63, and 77). The

158 mixing ratios of ammonium (NH_4^+ , m/z 18) and polycyclic aromatic hydrocarbons (e.g.,
159 m/z 116 ($[\text{C}_9\text{H}_8]^+$), 129 ($[\text{C}_{10}\text{H}_9]^+$), 140 ($[\text{C}_{11}\text{H}_8]^+$), and 153 ($[\text{C}_{12}\text{H}_9]^+$)) were higher in
160 winter than in summer. The strong signal of NH_4^+ was possibly due to the lower
161 temperature (8°C) in winter than in summer (31°C). The mixing ratios of m/z 59 were
162 45% and 44% during summer and winter, respectively.

163 In the negative mass spectra of two seasons (Figures 1(b) and 1(d)), the dominant ions
164 were CN^- (m/z -26), CNO^- (m/z -42), nitrate (m/z -46 and -62), phosphate (-79), and
165 sulfate (m/z -80 and -97). Primary species, such as CN^- and CNO^- were commonly
166 from biomass burning (BB) and organonitrogen (Pratt et al., 2011). Levoglucosan
167 markers from BB, such as -45, -59, and -71 were also detected. Dust markers, such as
168 $[\text{SiO}_2]^-$ (m/z -60), $[\text{}^{28}\text{SiO}_3]^-$ or $[\text{AlO}_2(\text{OH})]^-$ (-76), and $[\text{PO}_3]^-$, were also detected during
169 summertime, suggesting the influence of dust particles.

170 Prior to comparison, the ion peak was normalized using the method developed by Qin
171 et al. (2012). Briefly, the peak area of each m/z was divided by the total mass spectral
172 peak area matrix. The normalized ion intensity of the wintertime particles was
173 subtracted from that of the summertime particles. A positive value indicates the
174 normalized ion intensity was greater in the summer, whereas a negative value indicates
175 that the normalized ion intensity was greater in the winter. As shown in Figure S3, Ca^+
176 (m/z 40) and Fe^+ (m/z 56) were more prevalent during summer. Organic species, such
177 as C_2H_3^+ (m/z 27), C_4H_3^+ (m/z 51), C_5H_3^+ (m/z 63), and C_6H_5^+ (m/z 77) typically from
178 aromatic hydrocarbons, were also more abundant in summer. During wintertime,
179 signals of sulfate (m/z -97), NO_3^- (m/z -62), NH_4^+ (m/z 18), and K^+ (m/z 39) were more
180 prominent than in summer, suggesting that the wintertime particles contained more
181 secondary species than those in summer.

182 The unscaled size distribution of amine-containing particles also showed strong
 183 seasonal variations (Figure S4). Generally, amine-containing particles had monomodal
 184 size distributions in the droplet mode; and the distributions peaked at a larger D_{va} in
 185 summer than winter. For example, DEA-containing particles peaked at 0.6 μm in winter
 186 and 0.8 μm in summer, and DPA-containing particles at 0.7 μm in winter and 0.9 μm
 187 in summer. The size distributions of the major amine-containing particles suggested
 188 that these particles had undergone substantial aging processes.



189

190 Figure 1. (a) and (c): the positive digital mass spectrum of amine-containing particles
 191 during summer and wintertime, respectively; (b) and (d): the negative digital mass
 192 spectrum during summer and wintertime, respectively. The ion height indicates its
 193 fraction in the amine-containing particle dataset, and the stacked color map indicates
 194 the ion peak area range.

195 3.2 Temporal trend, diurnal pattern, and origin of amine-containing particles

196 Figure 2 shows the temporal trends of RH, temperature, number count, and the peak area
197 of amine-containing particles. The winter temperature was lower ($8.0\pm 4.0^\circ\text{C}$) than
198 summer ($31\pm 4^\circ\text{C}$), and RH in the winter was slightly higher ($70\pm 14\%$ versus $64\pm 16\%$)
199 (Table 1). Stagnant air conditions occurred in both seasons due to the low wind speeds
200 (Huang et al., 2017), and the winter wind speed was lower than in summer. The hourly
201 count of amine-containing particles was typically ten times higher in winter than
202 summer.

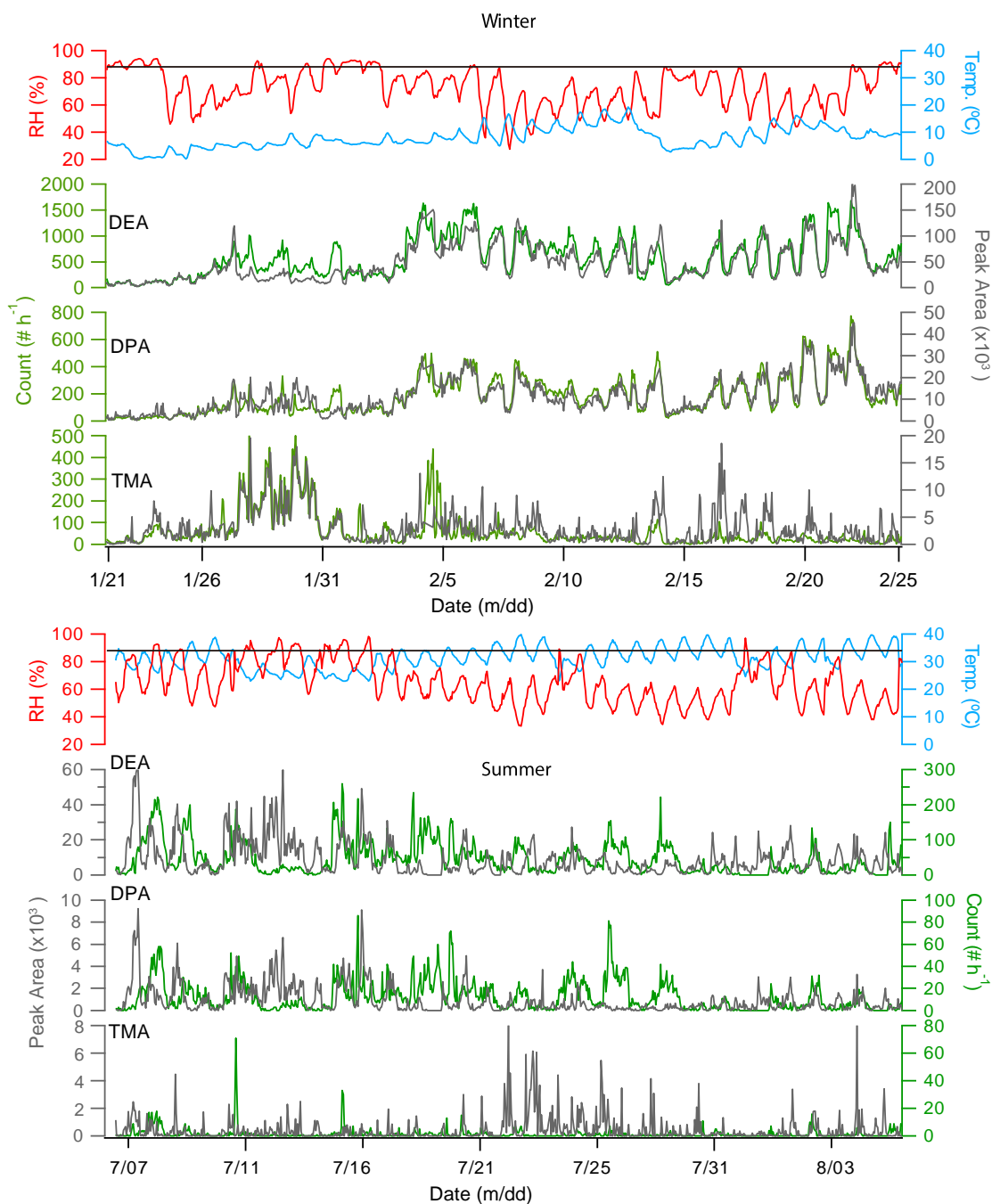
203 In winter, a good correlation existed between the temporal trends of hourly number
204 count and peak area of DEA-containing particles ($R^2 = 0.86$). The corresponding R^2 in
205 wintertime DPA-containing particles was 0.88. No such correlation for TMA-
206 containing particles was observed in winter ($R^2 = 0.22$) or summer (Figure 2). The
207 hourly counts of DEA- and DPA-containing particles were well correlated in both
208 summer ($R^2 = 0.63$) and winter ($R^2 = 0.87$), but a weak correlation ($R^2 = 0.25$) existed
209 between DEA- and TMA-containing particles. These results suggest DEA- and DPA-
210 containing particles were possibly from the same sources.

211 Table 1. Meteorological factors and particle counts in summer and winter.

	Winter	Summer
212		
213	Temperature ($^\circ\text{C}$)	8 ± 4 31 ± 4
	Relative humidity (%)	70 ± 14 64 ± 16
214	Wind Speed	1.2 ± 0.7 1.5 ± 1.0
215	Amine-particle Count ($\# \text{ h}^{-1}$)	587 ± 384 47 ± 26

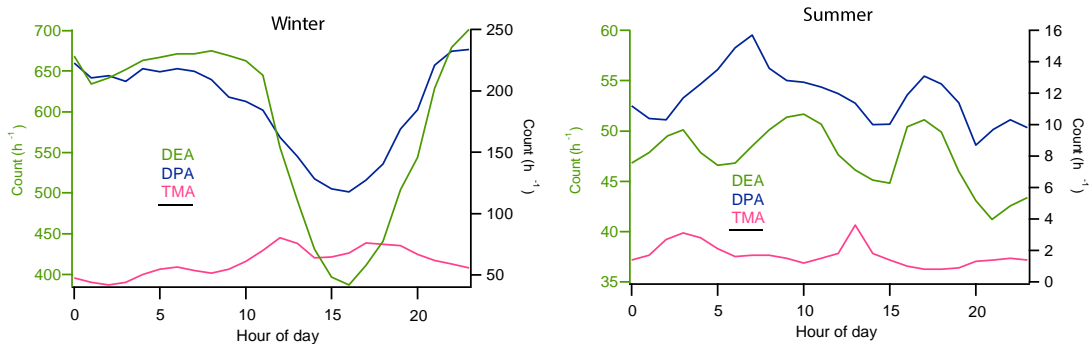
216 DEA- and DPA-containing particles remained at low levels from 1/20/2016 to
217 01/26/2016 and averaged at 109 and 26 count h⁻¹, respectively. During this period, wind
218 speed was relatively high, commonly above 1.5 ms⁻¹. TMA-, DEA-, and DPA-
219 containing particles started accumulating after 01/26/2016 when wind speed was low
220 (0.8 ms⁻¹) and wind direction from the northwest. After 02/03/2016, DEA- and DPA-
221 containing particles showed regular diurnal patterns with high levels of hourly count
222 during daytime on most days and minimum levels at 15:00. A similar diurnal pattern
223 was also observed for DPA-containing particles during wintertime (Figures 3). TMA-
224 containing particles presented a complex diurnal profile with peaks in the early morning
225 (4:00), at noon (12:00) and in the afternoon (18:00). The chemical composition and
226 diurnal pattern of TMA-containing particles were strongly connected to traffic
227 emissions.

228 Wind direction and number count of amine-containing particles were analyzed together
229 using bivariate polar plots (Figure 4). During wintertime, the dominant direction for
230 amine-containing particles was from the northwest where a forest park was located.
231 After being emitted from vegetation (plants, grass, and trees) (Ge et al., 2011a), DEA
232 could partition to the pre-existing particles before arriving at the sampling site. The
233 transport of these particles to the sampling site caused the elevation in the morning.
234 Based on the excellent correlation between DEA- and DPA-containing particles, DPA-
235 containing particles could also be from vegetation. It can be concluded that the major
236 source of amines in DEA- and DPA-containing particles was vegetation from the
237 northwest.



238

239 Figure 2. Temporal trends of relative humidity (RH), temperature (Temp.), hourly peak
 240 area (dark gray), and particle count (green) of DEA (m/z 74), DPA (m/z 86), and TMA
 241 (m/z 59) -containing particles in winter (top panel) and summer (bottom panel). The
 242 black lines in the two panels indicate RH of 90%.



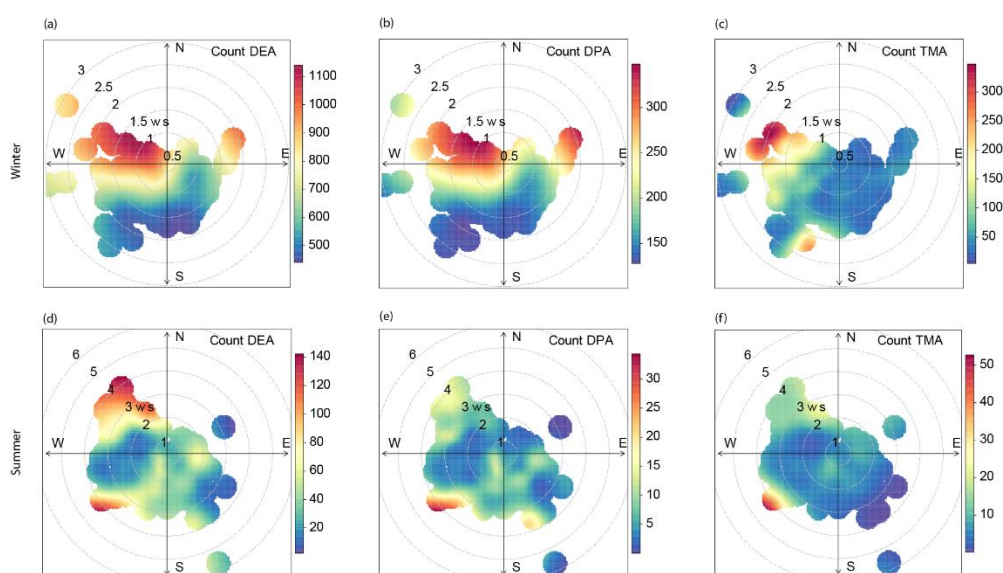
243

244 Figure 3. Diurnal profiles of amine-containing particles during both winter (left panel)
 245 and summer (right panel). The green left axis in each panel indicates the average
 246 number count of DEA-containing particles, while the right-axis represents the number
 247 count of both DPA- and TMA-containing particles.

248 During summer, the amine particles appeared in several episodes; each episode lasted
 249 for 1~3 days. In these episodes, DPA-containing particles had two rush-hour peaks
 250 (7:00 and 17:00), likely from traffic (Dall'Osto et al., 2016). Besides traffic, vegetation
 251 is also a source of DPA-containing particles (from the southwest, Figure 4e). The DPA-
 252 containing particles peaked 0.84 μm , suggesting that they were not freshly-emitted and
 253 had undergone substantial aging processes. Moreover, as shown in Figure S2, the mass
 254 spectra of the amines were present with aromatic hydrocarbon fragments, such as C_4H_3^+
 255 (m/z 51), C_5H_3^+ (m/z 63), C_6H_5^+ (m/z 77), and C_9H_8^+ (m/z 116), as well as with alkanes
 256 fragments such as C_4H_7^+ (m/z 55), C_4H_9^+ (m/z 57), and C_5H_9^+ (m/z 69). The chemical
 257 composition of DPA-containing particles contained markers associated with traffic
 258 emissions. Similar amine-containing particle type has been reported in the literature
 259 (Dall'Osto et al., 2016).

260 In summer, DEA-containing particles had a diurnal pattern of three peaks appearing at
 261 3:00, 9:00 and 17:00. TMA-containing particles had an early morning (4:00) and a noon
 262 peak (12:00). The morning peaks of DEA- and TMA-containing particles could be due

263 to the local traffic emissions; specifically, heavy-duty vehicles were only allowed to
264 enter the urban area between 00:00 and 6:00 (Chen et al., 2017). The polar plots showed
265 that DEA-containing particles were from the northwest and southwest, passing through
266 the forest park and traffic hub, respectively. This scenario seemed to be inconsistent
267 with the wintertime results because of the limited traffic contributions to particle levels
268 in winter. In addition, due to the competition between vegetation and traffic in summer,
269 the number count and peak area of all three amine-containing particles were poorly
270 correlated with each other.



271

272 Figure 4. Polar plots of amine-containing particles during winter- and summertime. The
273 axes in each figure indicate hourly count of each particle type and the colors within the
274 circles represent wind speed (ws)

275 3.3 Effect of RH on the enrichment of DEA-containing particles

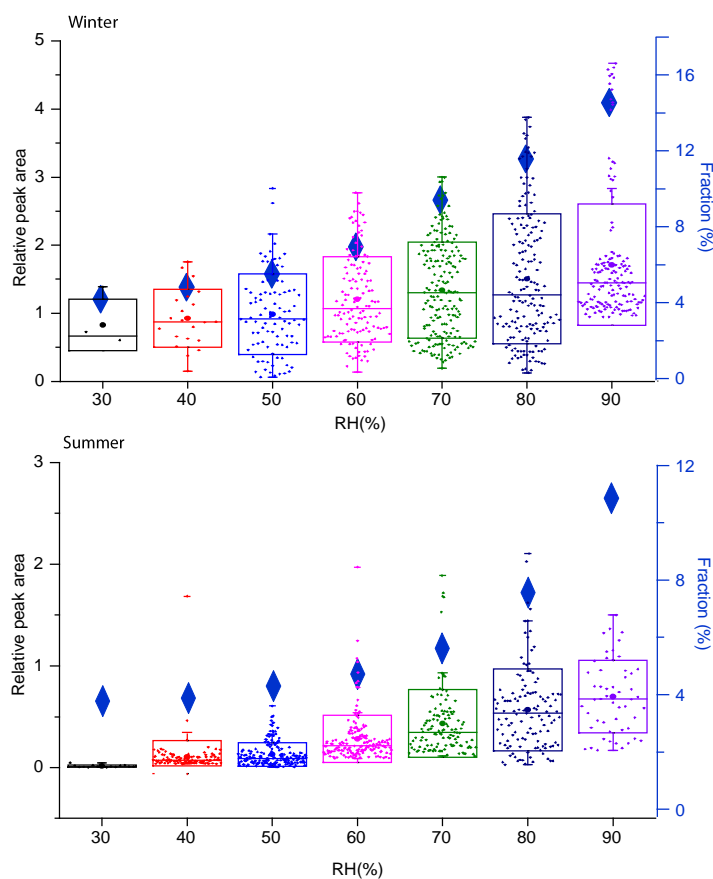
276 DEA-containing particles were predominant in both winter and summer, providing a
277 unique opportunity for investigating DEA processing. Indeed, [the effect of RH on](#)
278 [aerosol chemical processing](#) should be treated cautiously and the influences of wind

279 speed, wind direction, temperature, and planetary boundary layer reduction should be
280 removed. As described above, the average wind speed in both winter and summer was
281 1.2 ms^{-1} and 1.5 ms^{-1} , respectively. In these stagnant air conditions, the sampled
282 particles were generally local. Temperature could influence the gas-particle phase
283 partitioning. Assuming the Henry's Law constants (K_H) and the enthalpy change
284 $\Delta_r H_o(K_H)$ of DEA are constant, a variation of 10°C in both summer and winter has
285 negligible influence on the partitioning of amines from the gas phase to the particle
286 phase, according to the Clapeyron equation (Ge et al., 2011b). In addition, the shift in
287 planetary boundary layer (PBL) height could affect the number count and concentration
288 of PM. Using the temporal trends of RPA, the influence of PBL height can be removed
289 because it only shows the relative changes between different species which are all
290 simultaneously influenced by the shift in the PBL height.

291 Box plots of DEA relative peak area under different RH are shown in Figure 5. In winter,
292 the median RPA of amine-containing particles increased by two times when RH
293 increased from 35% to 95%. Meanwhile, the fraction of DEA-containing particles
294 increased from 4.0% to 16.6%. In summer, the average RPA of DEA increased by three
295 times (from 0.25 to 0.75) and the fraction of DEA-containing particles ramped from
296 3.8% to 12.1% when RH increased from 60% to 90%. These results suggest that RH is
297 important to the enrichment of DEA in the particle phase. [When DEA reacts with HCl,](#)
298 [H₂SO₄, and HNO₃, it tends to form aminium salts, which are soluble in aerosol water.](#)
299 Along with the influence of aerosol water content, Ge et al. (2011a) also proposed that
300 strong aerosol acidity could also enhance the partitioning of DEA in the aqueous phase.
301 [As particles are dried in the SPAMS, the amount of aerosol water content and pH were](#)
302 [unavailable. The values of the anion/ cation ratio \(\(sulfate +nitrate\)/ammonium, Yao et](#)
303 [al. \(2011\) were in a range of 20-150 suggesting that the particles might have been acidic](#)

304 which favors the dissolution of DEA. Overall, these results implied that high RH
305 conditions in Chongqing was favorable for particle uptake of DEA, and the resulting
306 formation of aminium salts stabilized pre-existing particles; thus, increased their
307 number concentrations.

308 Rehbein et al. (2011) and Zhang et al. (2012) observed direct links between fog
309 processing and enhancement of TMA-containing particles. High RH conditions were
310 favorable for TMA entering the particle phase via gas -particle partitioning (Rehbein et
311 al., 2011; Zhang et al., 2012). Ge et al. (2011b) argued that TMA in the aerosol phase
312 was in the form of free base, e.g., amine, not aminium salt; TMA could be dissolved in
313 the aerosol water; the formation of TMA-HSO₄ salt was possible, but the formation of
314 TMA-NO₃ and TMA-Cl was impossible due to the competition with ammonia. Thus,
315 TMA could enter the aerosol phase by gas-aqueous partitioning, or in the form of TMA-
316 HSO₄ salt. The mechanism of DEA entering the aerosol phase might be different from
317 TMA. DEA salts were favorable for forming in aerosol phase (Ge et al., 2011b).
318 Besides, Pankow (2015) proposed that the absorptive uptake of atmospheric amines
319 could also be possible on organic aerosols. In the context of single particle mixing state,
320 the amine-containing particles were internally mixed with hygroscopic species, e.g.,
321 sulfate, nitrate, POA species (C_xH_y⁺, see section 3.4), and SOA species (oxalate,
322 C₂H₃O⁺). Therefore, the mixing state of amine-containing particles was also favorable
323 for the uptake of amines via different pathways: the aqueous dissolution of aminium
324 salts and the absorptive uptake on OA.



325

326 Figure 5. Box plots of the hourly relative peak area of DEA under different RH
 327 conditions in winter (top panel) and summer (bottom panel). The boxes indicate the
 328 25th and 75th percentiles; the dots indicate mean value with each data point representing
 329 a datum of RPA in an hour size bin. Right axis in each panel and the blue diamonds
 330 show the average number fraction of amine-containing particles among the whole
 331 [SPAMS](#) dataset.

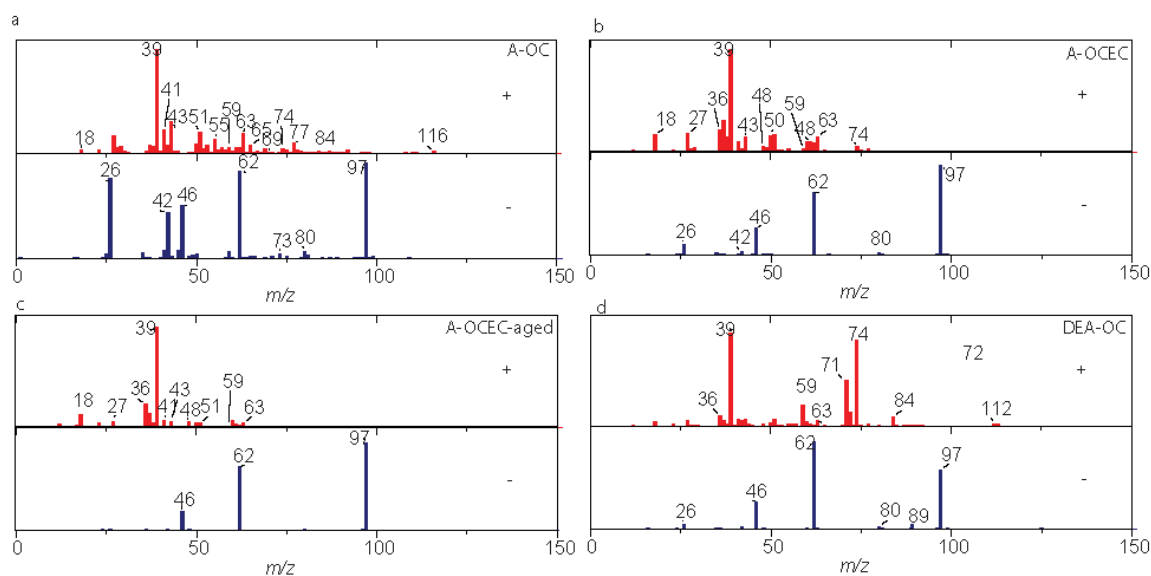
332 3.4 Particle types of amine-containing particles

333 As shown in Figure 6, four amine-containing particle types were resolved, including
 334 amine-OC (A-OC, 41%), A-ECOC (39%), DEA-OC (11%), and A-ECOC-aged (9%).
 335 All of these particle types had strong signals of amines, and the amines were internally
 336 mixed with sulfate, nitrate, elemental carbon, and organics.

337 In the A-OC particles, amines were mixed with aromatic hydrocarbon fragments, such
338 as $C_4H_3^+$ (m/z 51), $C_5H_3^+$ (m/z 63), $C_6H_5^+$ (m/z 77), and $C_9H_8^+$ (m/z 116), as well as with
339 alkanes fragments such as $C_4H_7^+$ (m/z 55), $C_4H_9^+$ (m/z 57), and $C_5H_9^+$ (m/z 69). In the
340 negative mass spectrum of A-OC, strong signals from CN^- (m/z -26) and CNO^- (m/z
341 -42) were typically primary species, along with levoglucosan (Silva et al., 1999). The
342 amine fragments, such as TMA (m/z 59), DEA (m/z 74), and DPA (m/z 86), were very
343 abundant in this particle type (76%, 95%, and 88%, respectively). The parent particles
344 of A-OC were a kind of OC particles from biomass burning; then they mixed with
345 amines via uptake. Amines could enter the A-OC particle type via dissolution in the
346 aerosol water content or uptake due to absorptive uptake on the organic aerosol
347 (Pankow, 2015).

348 In A-ECOC mass spectra, strong signals of amines (m/z 59 and 74), along with the
349 major aromatic hydrocarbon fragments and EC components (i.e., m/z 36, 48, 60) were
350 detected. In the negative mass spectra, nitrate and sulfate were also dominant. The A-
351 ECOC-aged particle type had a similar chemical composition to A-ECOC ($R^2=0.53$)
352 but with weaker relative intensities of $C_xH_y^+$ and amine ions, suggesting it could be
353 more secondary.

354 In the positive mass spectra of DEA-OC, DEA fragment (m/z 74) was dominant and
355 present with organic fragments described above. The secondary organic marker ions,
356 such as m/z 43 ($[C_2H_3O]^+$) and -89 (oxalic acid), were found in the mass spectra.
357 Besides, DEA-OC was not sensitive to wind speed ($R^2=0.18$), implying they were local.



358

359 Figure 6. Average mass spectra of major particle types clustered from amine-containing
 360 particles.

361 The summertime amine-containing particles were similar to the particle types during
 362 winter (all $R^2 > 0.7$), except a Ca-rich particle type was also resolved (Figure S5). A-
 363 Ca-OC particle type was mainly composed of calcium (Ca^+ and CaO^+), sodium (m/z
 364 23), potassium (m/z 39), TMA (m/z 59), sulfate, nitrate, and phosphate. An ion signal
 365 of zinc (m/z 64) was observed in the positive mass spectrum. Zn is a marker for tire
 366 wear on roads (Grigoratos and Martini, 2015; Thorpe and Harrison, 2008). The A-Ca-
 367 OC particle type was possibly from traffic activities (Chen et al., 2017).

368 The amine-containing particle types reported in this study were different from those in
 369 literature. Cheng et al. (2018) reported that m/z 74 amine-containing particles were most
 370 abundant in the Pearl River Delta, China, but the chemical composition and mixing
 371 state of amine particles were different from this study. For example, the mixing ratio of
 372 DPA was much stronger (~ 0.2) in Guangdong than in Chongqing (< 0.1). In most related
 373 studies, TMA-containing particles were dominant, while the present study showed

374 DEA-containing particles were dominant (Rehbein et al., 2011; Zhang et al., 2012;
375 Healy et al., 2015; Dall'Osto et al., 2016).

376 **4. Conclusions**

377 Amine-containing particles were collected and analyzed during winter and summer in
378 the urban area of Chongqing. Generally, amine-containing particles were more
379 abundant in winter than in summer. DEA-containing particles (m/z 74) were the most
380 important particle type during both summer and winter. Amines were internally mixed
381 with EC components, organics, sulfate, and nitrate, suggesting particle aging was
382 significant in both seasons. Amine-containing particles had monomodal size
383 distributions in the droplet mode, and the distributions peaked at a larger D_{va} in summer
384 than winter. DEA- and DPA-containing particles showed strong homogeneity, and
385 good correlations between the hourly number count and peak area were observed during
386 winter. The amine-containing particles were mostly from vegetation located southwest
387 of the sampling area, and traffic sources in the northwest. An enrichment of DEA-
388 containing particles under high RH conditions was revealed. Reduction of
389 anthropogenic amines, such as DEA and TMA, would improve the air quality in this
390 region, which can be achieved by decreasing the emissions of on-road fuel-powered
391 automobiles.

392 Acknowledgments. Financial support from the National Key Research and
393 Development Program of China (2018YFC0200403 and 2016YFC0201506), the
394 Nature Science Foundation of China (Grant No. 41375123), and the Educational
395 Commission of Sichuan Province of China (No: 15ZA0213) are acknowledged.

396 Author Contribution. CY and YF designed the experiments; TM, SG, PC, WH, and WQ
397 carried them out; HR, CY, ZL, CJ, and GD analyzed the experiment data; CY prepared
398 the manuscript with contributions from all co-authors.

399 **References**

400 Angelino, S., Suess, D. T., and Prather, K. A.: Formation of aerosol particles from
401 reactions of secondary and tertiary alkylamines: characterization by aerosol time-of-
402 flight mass spectrometry, *Environ Sci Technol*, 35, 3130-3138, 10.1021/es0015444,
403 2001.

404 Bzdek, B. R., Zordan, C. A., Pennington, M. R., Luther, G. W., 3rd, and Johnston, M.
405 V.: Quantitative assessment of the sulfuric acid contribution to new particle growth,
406 *Environ Sci Technol*, 46, 4365-4373, 10.1021/es204556c, 2012.

407 Chen, Y., Cao, J., Huang, R., Yang, F., Wang, Q., and Wang, Y.: Characterization,
408 mixing state, and evolution of urban single particles in Xi'an (China) during wintertime
409 haze days, *Sci Total Environ*, 573, 937-945, 10.1016/j.scitotenv.2016.08.151, 2016.

410 Chen, Y., Yang, F., Mi, T., Cao, J., Shi, G., Huang, R., Wang, H., Chen, J., Lou, S., and
411 Wang, Q.: Characterizing the composition and evolution of and urban particles in
412 Chongqing (China) during summertime, *Atmos Res*, 187, 84-94,
413 10.1016/j.atmosres.2016.12.005, 2017.

414 Cheng, C. L., Huang, Z. Z., Chan, C. K., Chu, Y. X., Li, M., Zhang, T., Ou, Y. B., Chen,
415 D. H., Cheng, P., Li, L., Gao, W., Huang, Z. X., Huang, B., Fu, Z., and Zhou, Z.:
416 Characteristics and mixing state of amine-containing particles at a rural site in the Pearl
417 River Delta, China, *Atmos Chem Phys*, 18, 9147-9159, 10.5194/acp-18-9147-2018,
418 2018.

419 Dall'Osto, M., Querol, X., Alastuey, A., Minguillon, M. C., Alier, M., Amato, F., Brines,
420 M., Cusack, M., Grimalt, J. O., Karanasiou, A., Moreno, T., Pandolfi, M., Pey, J., Reche,
421 C., Ripoll, A., Tauler, R., Van Drooge, B. L., Viana, M., Harrison, R. M., Gietl, J.,
422 Beddows, D., Bloss, W., O'Dowd, C., Ceburnis, D., Martucci, G., Ng, N. L., Worsnop,
423 D., Wenger, J., Mc Gillicuddy, E., Sodeau, J., Healy, R., Lucarelli, F., Nava, S.,
424 Jimenez, J. L., Gomez Moreno, F., Artinano, B., Prévôt, A. S. H., Pfaffenberger, L.,
425 Frey, S., Wilsenack, F., Casabona, D., Jiménez-Guerrero, P., Gross, D., and Cots, N.:
426 Presenting SAPUSS: Solving Aerosol Problem by Using Synergistic Strategies in
427 Barcelona, Spain, *Atmos. Chem. Phys.*, 13, 8991-9019, 10.5194/acp-13-8991-2013,
428 2013.

429 Dall'Osto, M., Beddows, D. C. S., McGillicuddy, E. J., Esser-Gietl, J. K., Harrison, R.
430 M., and Wenger, J. C.: On the simultaneous deployment of two single-particle mass
431 spectrometers at an urban background and a roadside site during SAPUSS, *Atmos*
432 *Chem Phys*, 16, 9693-9710, 10.5194/acp-16-9693-2016, 2016.

433 Dallosto, M., and Harrison, R.: Chemical characterisation of single airborne particles
434 in Athens (Greece) by ATOFMS, *Atmos Environ*, 40, 7614-7631,
435 10.1016/j.atmosenv.2006.06.053, 2006.

436 De Haan, D. O., Hawkins, L. N., Kononenko, J. A., Turley, J. J., Corrigan, A. L.,
437 Tolbert, M. A., and Jimenez, J. L.: Formation of nitrogen-containing oligomers by
438 methylglyoxal and amines in simulated evaporating cloud droplets, *Environ Sci*
439 *Technol*, 45, 984-991, 10.1021/es102933x, 2011.

440 Denkenberger, K. A., Moffet, R. C., Holecek, J. C., Rebotier, T. P., and Prather, K. A.:
441 Real-time, single-particle measurements of oligomers in aged ambient aerosol particles,
442 *Environ Sci Technol*, 41, 5439-5446, 10.1021/es070329l, 2007.

443 Ge, X., Wexler, A. S., and Clegg, S. L.: Atmospheric amines – Part I. A review, *Atmos*
444 *Environ*, 45, 524-546, 10.1016/j.atmosenv.2010.10.012, 2011a.

445 Ge, X., Wexler, A. S., and Clegg, S. L.: Atmospheric amines – Part II. Thermodynamic
446 properties and gas/particle partitioning, *Atmos Environ*, 45, 561-577,
447 10.1016/j.atmosenv.2010.10.013, 2011b.

448 Gómez Alvarez, E., Viidanoja, J., Muñoz, A., Wirtz, K., and Hjorth, J.: Experimental
449 Confirmation of the Dicarbonyl Route in the Photo-oxidation of Toluene and Benzene,
450 *Environ Sci Technol*, 41, 8362-8369, 10.1021/es0713274, 2007.

451 Grigoratos, T., and Martini, G.: Brake wear particle emissions: a review, *Environ Sci*
452 *Pollut Res Int*, 22, 2491-2504, 10.1007/s11356-014-3696-8, 2015.

453 Healy, R. M., Sciare, J., Poulain, L., Crippa, M., Wiedensohler, A., Prevot, A. S. H.,
454 Baltensperger, U., Sarda-Estève, R., McGuire, M. L., Jeong, C. H., McGillicuddy, E.,
455 O'Connor, I. P., Sodeau, J. R., Evans, G. J., and Wenger, J. C.: Quantitative
456 determination of carbonaceous particle mixing state in Paris using single-particle mass
457 spectrometer and aerosol mass spectrometer measurements, *Atmos Chem Phys*, 13,
458 9479-9496, 10.5194/acp-13-9479-2013, 2013.

459 Healy, R. M., Evans, G. J., Murphy, M., Sierau, B., Arndt, J., McGillicuddy, E.,
460 O'Connor, I. P., Sodeau, J. R., and Wenger, J. C.: Single-particle speciation of
461 alkylamines in ambient aerosol at five European sites, *Anal Bioanal Chem*, 407, 5899-
462 5909, 10.1007/s00216-014-8092-1, 2015.

463 Huang, Q., Cai, X., Song, Y., and Zhu, T.: Air stagnation in China (1985–2014):
464 climatological mean features and trends, *Atmos. Chem. Phys.*, 17, 7793-7805,
465 10.5194/acp-17-7793-2017, 2017.

466 Huang, Y., Chen, H., Wang, L., Yang, X., and Chen, J.: Single particle analysis of
467 amines in ambient aerosol in Shanghai, *Environ Chem*, 9, 202-210, 10.1071/en11145,
468 2012.

469 Kirkby, J., Curtius, J., Almeida, J., Dunne, E., Duplissy, J., Ehrhart, S., Franchin, A.,
470 Gagne, S., Ickes, L., Kurten, A., Kupc, A., Metzger, A., Riccobono, F., Rondo, L.,
471 Schobesberger, S., Tsagkogeorgas, G., Wimmer, D., Amorim, A., Bianchi, F.,
472 Breitenlechner, M., David, A., Dommen, J., Downard, A., Ehn, M., Flagan, R. C.,
473 Haider, S., Hansel, A., Hauser, D., Jud, W., Junninen, H., Kreissl, F., Kvashin, A.,
474 Laaksonen, A., Lehtipalo, K., Lima, J., Lovejoy, E. R., Makhmutov, V., Mathot, S.,
475 Mikkila, J., Minginette, P., Mogo, S., Nieminen, T., Onnela, A., Pereira, P., Petaja, T.,
476 Schnitzhofer, R., Seinfeld, J. H., Sipila, M., Stozhkov, Y., Stratmann, F., Tome, A.,
477 Vanhanen, J., Viisanen, Y., Vrtala, A., Wagner, P. E., Walther, H., Weingartner, E.,
478 Wex, H., Winkler, P. M., Carslaw, K. S., Worsnop, D. R., Baltensperger, U., and
479 Kulmala, M.: Role of sulphuric acid, ammonia and galactic cosmic rays in atmospheric
480 aerosol nucleation, *Nature*, 476, 429-433, 10.1038/nature10343, 2011.

481 Li, L., Huang, Z., Dong, J., Li, M., Gao, W., Nian, H., Fu, Z., Zhang, G., Bi, X., Cheng,
482 P., and Zhou, Z.: Real time bipolar time-of-flight mass spectrometer for analyzing
483 single aerosol particles, *Int J Mass Spectrom*, 303, 118-124,
484 10.1016/j.ijms.2011.01.017, 2011.

485 Li, Y. J., Sun, Y., Zhang, Q., Li, X., Li, M., Zhou, Z., and Chan, C. K.: Real-time
486 chemical characterization of atmospheric particulate matter in China: A review, *Atmos*
487 *Environ*, 2017.

488 Moffet, R. C., de Foy, B., Molina, L. T., Molina, M. J., and Prather, K. A.: Measurement
489 of ambient aerosols in northern Mexico City by single particle mass spectrometry,
490 *Atmos. Chem. Phys.*, 8, 4499-4516, 10.5194/acp-8-4499-2008, 2008.

491 Monks, P. S.: Gas-phase radical chemistry in the troposphere, *Chem Soc Rev*, 34, 376-
492 395, 10.1039/b307982c, 2005.

493 Onasch, T. B., Trimborn, a., Fortner, E. C., Jayne, J. T., Kok, G. L., Williams, L. R.,
494 Davidovits, P., and Worsnop, D. R.: Soot Particle Aerosol Mass Spectrometer:
495 Development, Validation, and Initial Application, *Aerosol Sci. Technol.*, 46, 804-817,
496 10.1080/02786826.2012.663948, 2012.

497 Pankow, J. F.: Phase considerations in the gas/particle partitioning of organic amines
498 in the atmosphere, *Atmos Environ*, 122, 448-453, 10.1016/j.atmosenv.2015.09.056,
499 2015.

500 Pratt, K. A., Murphy, S. M., Subramanian, R., DeMott, P. J., Kok, G. L., Campos, T.,
501 Rogers, D. C., Prenni, A. J., Heymsfield, A. J., Seinfeld, J. H., and Prather, K. A.:
502 Flight-based chemical characterization of biomass burning aerosols within two
503 prescribed burn smoke plumes, *Atmos Chem Phys*, 11, 12549-12565, 10.5194/acp-11-
504 12549-2011, 2011.

505 Qin, X., Pratt, K. A., Shields, L. G., Toner, S. M., and Prather, K. A.: Seasonal
506 comparisons of single-particle chemical mixing state in Riverside, CA, *Atmos Environ*,
507 59, 587-596, 10.1016/j.atmosenv.2012.05.032, 2012.

508 Rehbein, P. J., Jeong, C. H., McGuire, M. L., Yao, X., Corbin, J. C., and Evans, G. J.:
509 Cloud and fog processing enhanced gas-to-particle partitioning of trimethylamine,
510 *Environ Sci Technol*, 45, 4346-4352, 10.1021/es1042113, 2011.

511 Silva, P. J., Liu, D.-Y., Noble, C. A., and Prather, K. A.: Size and Chemical
512 Characterization of Individual Particles Resulting from Biomass Burning of Local
513 Southern California Species, *Environ Sci Technol*, 33, 3068-3076, 10.1021/es980544p,
514 1999.

515 Smith, J. N., Barsanti, K. C., Friedli, H. R., Ehn, M., Kulmala, M., Collins, D. R.,
516 Scheckman, J. H., Williams, B. J., and McMurry, P. H.: Observations of aminium salts
517 in atmospheric nanoparticles and possible climatic implications, *Proc Natl Acad Sci U*
518 *S A*, 107, 6634-6639, 10.1073/pnas.0912127107, 2010.

519 Song, X. H., Hopke, P. K., Fergenson, D. P., and Prather, K. A.: Classification of single
520 particles analyzed by ATOFMS using an artificial neural network, ART-2A, *Anal.*
521 *Chem.*, 71, 860-865, DOI 10.1021/ac9809682, 1999.

522 Tan, P. V., Evans, G. J., Tsai, J., Owega, S., Fila, M. S., Malpica, O., and Brook, J. R.:
523 On-line analysis of urban particulate matter focusing on elevated wintertime aerosol
524 concentrations, *Environ Sci Technol*, 36, 3512-3518, 10.1021/es011448i, 2002.

525 Tao, J., Zhang, L., Cao, J., and Zhang, R.: A review of current knowledge concerning
526 PM_{2.5}; chemical composition, aerosol optical properties and
527 their relationships across China, *Atmos Chem Phys*, 17, 9485-9518, 10.5194/acp-17-
528 9485-2017, 2017.

529 Thorpe, A., and Harrison, R. M.: Sources and properties of non-exhaust particulate
530 matter from road traffic: a review, *Sci Total Environ*, 400, 270-282,
531 10.1016/j.scitotenv.2008.06.007, 2008.

532 Wang, J. F., Ge, X. L., Chen, Y. F., Shen, Y. F., Zhang, Q., Sun, Y. L., Xu, J. Z., Ge,
533 S., Yu, H., and Chen, M. D.: Highly time-resolved urban aerosol characteristics during

534 springtime in Yangtze River Delta, China: insights from soot particle aerosol mass
535 spectrometry, *Atmos Chem Phys*, 16, 9109-9127, 10.5194/acp-16-9109-2016, 2016.

536 Wang, L., Khalizov, A. F., Zheng, J., Xu, W., Ma, Y., Lal, V., and Zhang, R.:
537 Atmospheric nanoparticles formed from heterogeneous reactions of organics, *Nature*
538 *Geoscience*, 3, 238, 10.1038/ngeo778
539 <https://www.nature.com/articles/ngeo778#supplementary-information>, 2010.

540 Yao, L., Garmash, O., Bianchi, F., Zheng, J., Yan, C., Kontkanen, J., Junninen, H.,
541 Mazon, S. B., Ehn, M., Paasonen, P., Sipila, M., Wang, M., Wang, X., Xiao, S., Chen,
542 H., Lu, Y., Zhang, B., Wang, D., Fu, Q., Geng, F., Li, L., Wang, H., Qiao, L., Yang,
543 X., Chen, J., Kerminen, V. M., Petaja, T., Worsnop, D. R., Kulmala, M., and Wang, L.:
544 Atmospheric new particle formation from sulfuric acid and amines in a Chinese
545 megacity, *Science*, 361, 278-281, 10.1126/science.aao4839, 2018.

546 Yao, X., Rehbein, P. J. G., Lee, C. J., Evans, G. J., Corbin, J., and Jeong, C.-H.: A study
547 on the extent of neutralization of sulphate aerosol through laboratory and field
548 experiments using an ATOFMS and a GPIC, *Atmos Environ*, 45, 6251-6256,
549 10.1016/j.atmosenv.2011.06.061, 2011.

550 You, Y., Kanawade, V. P., de Gouw, J. A., Guenther, A. B., Madronich, S., Sierra-
551 Hernández, M. R., Lawler, M., Smith, J. N., Takahama, S., Ruggeri, G., Koss, A., Olson,
552 K., Baumann, K., Weber, R. J., Nenes, A., Guo, H., Edgerton, E. S., Porcelli, L., Brune,
553 W. H., Goldstein, A. H., and Lee, S. H.: Atmospheric amines and ammonia measured
554 with a chemical ionization mass spectrometer (CIMS), *Atmos. Chem. Phys.*, 14, 12181-
555 12194, 10.5194/acp-14-12181-2014, 2014.

556 Zhang, G., Bi, X., Chan, L. Y., Li, L., Wang, X., Feng, J., Sheng, G., Fu, J., Li, M., and
557 Zhou, Z.: Enhanced trimethylamine-containing particles during fog events detected by

558 single particle aerosol mass spectrometry in urban Guangzhou, China, Atmos Environ,
559 55, 121-126, 10.1016/j.atmosenv.2012.03.038, 2012.

560